Comment on "Commensurate-incommensurate transition and strain relief patterns in monolayer C_{60} on Cd(0001)"

Roman Forker and Torsten Fritz*
Friedrich-Schiller-Universität Jena, Institut für Festkörperphysik, Helmholtzweg 5, 07743 Jena, Germany

(Received 26 January 2022; accepted 12 July 2022; published 21 July 2022)

The assignment of epitaxy types by Wang *et al.* [Phys. Rev. B **103**, 245430 (2021)] is critically examined. In particular, a C_{60} phase grown on Cd(0001) is denoted by them as "incommensurate"; however, it is most likely higher order commensurate. The crucial distinction between these epitaxy types is discussed here. Further, the strain values given by Wang *et al.* with subpercent accuracy for C_{60} monolayers are revisited. Systematic errors are identified due to the unjustified negligence of the temperature dependencies of the involved lattice constants, the largest contribution stemming from the bulk lattice constant of C_{60} used by Wang *et al.* as a reference value for strain calculations.

DOI: 10.1103/PhysRevB.106.047401

In a recent paper, Wang *et al.* studied the interface between C_{60} and Cd(0001) [1]. For this purpose, they deposited nominally 10–15 monolayers (ML) of Cd onto a Si(111)-(7×7) substrate. Subsequently, they used the so-obtained Cd(0001) surface to grow ordered adlayers of C_{60} at various substrate temperatures between 200 and 330 K, which were then examined in a scanning tunneling microscope (STM) at $T_{\mathrm{STM}} = 77.6$ K.

Wang *et al.* reported an epitaxy matrix of $\left(\begin{smallmatrix} 7 & -3.5 \\ 3.5 & 10.4 \end{smallmatrix}\right)$ for a particular structure of C_{60} and called it "incommensurate." This claim has severe implications for the energetic stability, which is not *a priori* clear. The epitaxial energy gain of commensurate or higher order commensurate registries as well as "on-line coincidences" essentially stems from common periodicities between the adsorbate and substrate lattices [2] or, perhaps more intuitively, from the avoidance of energetically unfavorable adsorption sites [3]. However, for incommensurate epitaxial relations (provided that the adsorbate lattice is characterized by strict translational symmetry), there are no preferred adsorption sites within a substrate unit cell, and hence the energetic stability is by default unexplained [3]. The only satisfying theoretical concept proposed thus far invokes so-called static distortion waves, which were found experimentally for a different incommensurate system and whose decisive role for the epitaxial energy gain was demonstrated quantitatively [4]. To put it bluntly, the observation of an "incommensurate" epitaxial relation is an extraordinary claim, which therefore requires very robust evidence. For instance, one must be able to rule out epitaxy matrices consisting of four rational elements (with reasonably small denominators) and properly discuss experimental uncertainties. Further, incommensurate epitaxy implies that no coincidences $\vec{G}_{\mathrm{a}} \equiv \vec{G}_{\mathrm{s}}$ of reasonably low order can be found by means of surface-sensitive diffraction or Fourier-transformed STM images with sufficient resolution, which have to contain information on the underlying substrate. In such measurements, the occurrence or absence of coinciding spots would readily decide whether there is registry or not. Neither of the above was conclusively demonstrated in Ref. [1], which is why the asserted observation of an "incommensurate" phase is unsound. The qualitative distinction between incommensurability and epitaxy types involving coincidences [3] is explained in Appendix A.

Moreover, precise STM measurements are generally very demanding, because considerable uncertainties arise mainly due to calibration issues and shearing or stretching of STM images caused by lateral drift, which affects the slow and fast scanning directions differently. The fact that the epitaxy matrix elements were provided in Ref. [1] with a precision of one decimal place implies that the uncertainties are at least ±0.1 each. The above epitaxy matrix could therefore be rounded to $\left(\begin{smallmatrix} 7 & -3.5 \\ 3.5 & 10.5 \end{smallmatrix}\right)$, which is an allowed solution within an error margin of 1% (i.e., well within the realistic accuracy of STM measurements). In doing so, one can identify a 2×2 commensurate C_{60} supercell on Cd(0001) in this case, which justifies the assignment of the epitaxy type as higher order commensurate (HOC) instead of "incommensurate." Even if one uses the originally reported epitaxy matrix, the epitaxy type is not incommensurate, as we clarify in Appendix A. Thus, their central claim of a "commensurate-incommensurate transition" is unsubstantiated.

To demonstrate the role of uncertainties, Fig. 1 displays the alleged "incommensurate" C_{60} unit cell with the lattice constants $|\vec{a}_1| = |\vec{a}_2| = 27.6(1)$ Å and a domain angle $\theta = 19^\circ$ as published by Wang *et al.* [1]. Regrettably, the uncertainty for θ was not provided in Ref. [1]. Figure 1 also contains an alternative C_{60} unit cell proposed by us with the epitaxy matrix $\left(\begin{smallmatrix} 7 & 3.5 \\ -3.5 & 10.5 \end{smallmatrix}\right)$ using the Cd(0001) lattice constant of 2.969 Å as comprehensibly derived in Appendix B, scenario (i). This matrix was adapted to a 60° unit cell (instead of 120°) for the Cd(0001) surface to facilitate the comparison with the

---

*torsten.fritz@uni-jena.de

2469-9950/2022/106(4)/047401(5)

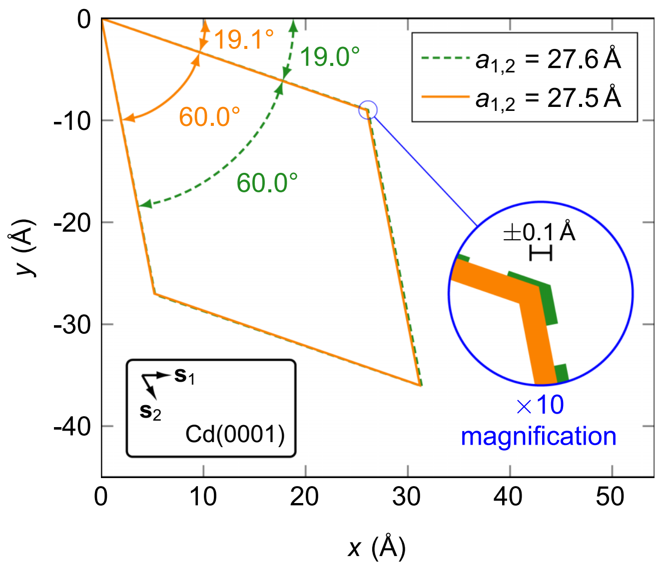

FIG. 1. Alleged "incommensurate" C_{60} unit cell as published by Wang *et al.* (green dashed lines). The orange solid lines depict an alternative C_{60} unit cell with the epitaxy matrix $\begin{pmatrix} 7 & 3.5 \\ -3.5 & 10.5 \end{pmatrix}$ using the Cd(0001) lattice constant of 2.969 Å as comprehensibly derived in Appendix B, scenario (i). This matrix was adapted to a 60° unit cell (instead of 120°) for the Cd(0001) surface to facilitate the comparison with the conventions used in Ref. [1]. The blue circular inset is a closeup view with a magnification factor of 10. Within the given uncertainty of ±0.1 Å, both C_{60} unit cells are indistinguishable.

conventions used in Ref. [1]. In this scenario, we obtain a hexagonal C_{60} unit cell with $|\vec{a}_1| = |\vec{a}_2| = 27.5$ Å and $\theta = 19.1^\circ$. Within the uncertainty of ±0.1 Å given by Wang *et al.*, their C_{60} unit cell is indistinguishable from our alternative. Importantly, this experimental uncertainty does not allow to rule out an HOC registry as given by our proposed epitaxy matrix that consists of four integer or half-integer elements.

Further, strain is discussed in Ref. [1]. For instance, a value of −1.2% is specified for another phase of C_{60}; see Eq. (B2). This implies an unrealistic *subpercent* accuracy of their STM measurements. If such experimental accuracies are claimed, then one also needs to account for thermal expansion, especially when using reference values in the calculations. While Wang *et al.* measured their structural parameters at 77.6 K in the STM [1], they used a reference value for the C_{60} bulk lattice constant a_{C60} valid at 300 K [5]. This implicit negligence of the temperature dependence of a_{C60} is a conceptual problem (thermal expansion is omitted without proper justification), and this disregard alone introduces an absolute error of ≈ 0.8–0.9% for all strain values; see Appendix B.

For the benefit of the reader, the temperature dependencies of the involved materials are scrutinized in Appendix B, including a discussion of two possible scenarios for the role of the substrate. There, we take the available temperature dependence of the C_{60} bulk lattice constant into account [6]. Based on those considerations, we compile the lattice parameters and the revised strain values in Table I. For the example of the HOC (10 × 10) structure, we conclude that more realistic strain values in the C_{60} monolayer are either −0.4% (i.e., slightly compressive) or +0.2% (i.e., slightly tensile), depending on the actual lattice constants of Cd(0001) and the role of the Si(111)-(7 × 7) substrate. The absolute values in both cases are one-third or less of the strain given in Ref. [1] for this C_{60} structure (−1.2%). Hence, in their example there is likely no significant strain at all.

Note that the rounded values of the lattice constants and the angles in Table I may still be unrealistically precise considering the typical uncertainties of STM measurements mentioned above. However, a reliable estimation of the accuracy of those

TABLE I. Lattice parameters for the Cd(0001) surface considering both scenarios (i) and (ii) detailed in the Appendixes. For two different C_{60} adlayer structures, described by Wang *et al.* as HOC (10 × 10) and "incommensurate," respectively, the lattice parameters are calculated based on the epitaxial relations given in Ref. [1]. The strain is calculated for the HOC (10 × 10) structure only, since the "incommensurate" structure exhibits apparently a nonuniform distribution of intermolecular distances as pointed out already in Ref. [1]. All values compiled here refer to a measurement temperature of 77.6 K. $\Gamma = \measuredangle(\vec{a}_1, \vec{a}_2)$ is the unit cell angle, and $\theta = \measuredangle(\vec{s}_1, \vec{a}_1)$ is the domain angle. Positive (negative) angles denote counterclockwise (clockwise) rotations.

Case	Description	$\lvert\vec{a}_1\rvert$ (Å)	$\lvert\vec{a}_2\rvert$ (Å)	Γ (deg)	θ (deg)	Epitaxy matrix **M**	Strain[a] e
A	Cd(0001) assuming scenario (i)	2.969(2)	2.969(2)	120			
B	Cd(0001) assuming scenario (ii)	2.98626(2)	2.98626(2)	120			
C	HOC (10 × 10) w.r.t. case A	29.69[b]	29.69[b]	120	0	$\begin{pmatrix} 10 & 0 \\ 0 & 10 \end{pmatrix}$	−0.4%
D	HOC (10 × 10) w.r.t. case B	29.86[b]	29.86[b]	120	0	$\begin{pmatrix} 10 & 0 \\ 0 & 10 \end{pmatrix}$	+0.2%
E	"incommensurate" w.r.t. case A	27.50[b]	27.22[b]	119.8[c]	−19.1[c]	$\begin{pmatrix} 7 & -3.5 \\ 3.5 & 10.4 \end{pmatrix}$	
E_{HOC}	same as E, but with HOC registry	27.50[b]	27.50[b]	120.0[c]	−19.1[c]	$\begin{pmatrix} 7 & -3.5 \\ 3.5 & 10.5 \end{pmatrix}$	
F	"incommensurate" w.r.t. case B	27.65[b]	27.37[b]	119.8[c]	−19.1[c]	$\begin{pmatrix} 7 & -3.5 \\ 3.5 & 10.4 \end{pmatrix}$	
F_{HOC}	same as F, but with HOC registry	27.65[b]	27.65[b]	120.0[c]	−19.1[c]	$\begin{pmatrix} 7 & -3.5 \\ 3.5 & 10.5 \end{pmatrix}$	

[a] Using Eq. (B2) and $d_{NN,bulk} = a_{C60}/\sqrt{2}$ with $a_{C60} = 14.05(1)$ Å from Fig. 2.

[b] The values for the C_{60} adlayer lattice constants are rounded to two decimal places each; see the text.

[c] The values for the unit cell angle Γ and the domain angle θ are rounded to one decimal place each; see the text.

values would require knowledge of reasonable experimental uncertainties for the epitaxy matrix elements, which were not provided in Ref. [1].

In conclusion, the structure with the nominal epitaxy matrix $\left(\begin{smallmatrix}7 & -3.5\\ 3.5 & 10.4\end{smallmatrix}\right)$ given by Wang *et al.* is most likely not incommensurate but HOC. We propose surface-sensitive diffraction methods, such as distortion-corrected low-energy electron diffraction (LEED) [7], to assign the epitaxy type with better confidence. For incommensurate phases, in particular, one expects additional satellite diffraction spots due to multiple scattering, which greatly improves the accuracy of the determined epitaxial relation as we and others have previously demonstrated [4,8–10]. Moreover, the strain values in Ref. [1] are found to contain sizable systematic errors due to the unjustified negligence of the thermal expansion of the involved materials. Most notably, the nearest-neighbor distance for C_{60} bulk crystals at 77.6 K [6] should be used as a reference for strain calculations.

We acknowledge funding by the Deutsche Forschungsgemeinschaft (DFG) through Grant No. FR 875/19-1. Further, we thank the anonymous reviewer for helpful recommendations.

APPENDIX A: ASSIGNMENT OF EPITAXY TYPES

For the assignment of epitaxy types it is useful to relate the adsorbate lattice vectors $\vec{a}_1$, $\vec{a}_2$ to the substrate lattice vectors $\vec{s}_1$, $\vec{s}_2$ by means of an epitaxy matrix $\mathbf{M}$:

$$\begin{pmatrix}\vec{a}_1\\ \vec{a}_2\end{pmatrix} = \mathbf{M}\cdot\begin{pmatrix}\vec{s}_1\\ \vec{s}_2\end{pmatrix} \quad \text{with } \mathbf{M} = \begin{pmatrix}M_{11} & M_{12}\\ M_{21} & M_{22}\end{pmatrix}. \tag{A1}$$

This definition is to be understood as

$$\vec{a}_1 = M_{11}\cdot\vec{s}_1 + M_{12}\cdot\vec{s}_2, \tag{A2}$$

$$\vec{a}_2 = M_{21}\cdot\vec{s}_1 + M_{22}\cdot\vec{s}_2. \tag{A3}$$

The common nomenclature for a matrix $\mathbf{M}$ consisting of four integer elements is a commensurate epitaxial registry. It is straightforward to show that if $\mathbf{M}$ consists of four rational elements, then one can find a commensurate supercell for the adsorbate lattice (in the simplest case using integer multiples of $\vec{a}_1$ and $\vec{a}_2$ as the new lattice vectors) [3]. This epitaxy type is dubbed higher order commensurate (HOC), because in this case a *nonprimitive* adsorbate unit cell (instead of a *primitive* adsorbate unit cell) can be described by four integer epitaxy matrix elements with respect to the substrate lattice. Commensurate and HOC epitaxial registries share the same qualitative characteristic, namely that one can find common periodicities of the adsorbate and the substrate lattices in two linearly independent directions.

In reciprocal space, a common periodicity is equivalently described by a so-called coincidence, i.e., by an identity of the reciprocal lattice vectors of the adsorbate $\vec{G}_\mathrm{a}$ and the substrate $\vec{G}_\mathrm{s}$ (in a specific direction) [3]:

$$h_\mathrm{a}\cdot\vec{a}_1^* + k_\mathrm{a}\cdot\vec{a}_2^* = \vec{G}_\mathrm{a} \equiv \vec{G}_\mathrm{s} = h_\mathrm{s}\cdot\vec{s}_1^* + k_\mathrm{s}\cdot\vec{s}_2^*. \tag{A4}$$

Importantly, it is shown in Ref. [3] that if such a coincidence (A4) exists, then its integer orders h_a, k_a and h_s, k_s are related by the *same* epitaxy matrix as in Eq. (A1):

$$\begin{pmatrix}h_\mathrm{a}\\ k_\mathrm{a}\end{pmatrix} = \mathbf{M}\cdot\begin{pmatrix}h_\mathrm{s}\\ k_\mathrm{s}\end{pmatrix} \quad \text{with } \mathbf{M} = \begin{pmatrix}M_{11} & M_{12}\\ M_{21} & M_{22}\end{pmatrix}. \tag{A5}$$

In Table I we list two different C_{60} adlayer structures as described in Ref. [1]. The structure called HOC (10 × 10) contains nine molecules per nonprimitive unit cell and is characterized by a fully integer epitaxy matrix; the primitive unit cell is indeed attributable to a higher order commensurate registry as one may infer from the molecular arrangement visualized by means of STM [1]. Hence, the assignment to the HOC epitaxy type is plausible.

The structure dubbed "incommensurate" by Wang *et al.*, however, very likely obeys an HOC epitaxial registry as well. The epitaxy matrix provided in Ref. [1] fulfills a coincidence of reasonably small order $(h_\mathrm{s}, k_\mathrm{s}) = (2, 0)$:

$$\begin{pmatrix}14\\ 7\end{pmatrix} = \begin{pmatrix}7 & -3.5\\ 3.5 & 10.4\end{pmatrix}\begin{pmatrix}2\\ 0\end{pmatrix}. \tag{A6}$$

The Cd(0001) substrate is hexagonal, as is likely also the case for the $\left(\begin{smallmatrix}7 & -3.5\\ 3.5 & 10.4\end{smallmatrix}\right)$ structure of C_{60}. With these four epitaxy matrix elements, one computes a unit cell angle of $\Gamma = 119.8^\circ$. The difference from 120.0° is *not* significant, especially considering the typical experimental uncertainties in STM, as mentioned above. Therefore, it is very likely that this structure found by Wang *et al.* is in fact also hexagonal. The implication of this circumstance is that if one finds a coincidence for a hexagonal adsorbate lattice on a hexagonal substrate lattice [as we did in Eq. (A6)], then one automatically obtains a second coincidence rotated by either 60° or 120°. This means in turn that one has two linearly independent coincidences, which is equivalent to an HOC epitaxial registry [3]. Consequently, the $\left(\begin{smallmatrix}7 & -3.5\\ 3.5 & 10.4\end{smallmatrix}\right)$ structure of C_{60} on Cd(0001) constitutes most likely also a higher order commensurate registry, and calling it "incommensurate" is not sufficiently supported by experimental evidence.

APPENDIX B: DISCUSSION OF STRAIN

Wang *et al.* discuss the effects of strain in C_{60} monolayers by comparing the measured intermolecular distance, which shall be called $d_\mathrm{NN,film}$ here, to the nearest-neighbor distance $d_\mathrm{NN,bulk}$ in C_{60} bulk samples. Linear strain e can be defined for small deformations as

$$e = \frac{d_\mathrm{NN,film} - d_\mathrm{NN,bulk}}{d_\mathrm{NN,bulk}} = \frac{d_\mathrm{NN,film}}{d_\mathrm{NN,bulk}} - 1. \tag{B1}$$

For a specific C_{60} monolayer sample deposited at 200 K, Wang *et al.* characterize the adlayer structure (with nine molecules per unit cell) to form a 10 × 10 registry with the Cd(0001) surface. For the latter, they indicate a lattice constant of 2.97 Å, referring to a previous report [11]. The distance 10 × 2.97 Å is then related to $3 \times d_{\text{NN,bulk}}$ with $d_{\text{NN,bulk}} = 10.02$ Å taken from the literature [5]:

$$e = \frac{10 \times 2.97\ \text{Å}}{3 \times 10.02\ \text{Å}} - 1 = -1.2\%. \tag{B2}$$

The above is meant to reconstruct the calculations made by Wang *et al.* However, in the following we raise concerns about the lengths used in Eq. (B2), which lead to the strain values reported in Ref. [1].

Temperature-dependence of the cubic lattice constant of bulk C_{60}

For the cubic lattice constant of bulk C_{60}, Wang *et al.* used a value of $a = 14.17(1)$ Å [5], resulting in a nearest-neighbor distance of $d_{\text{NN,bulk}} = a/\sqrt{2} = 10.02(1)$ Å. This value, however, is valid for $T = 300$ K. In the same paper by Heiney *et al.*, another value of $a = 14.04(1)$ Å is given for $T = 11$ K [5], which clearly demonstrates that the C_{60} crystals are subject to non-negligible thermal expansion. Figure 2 depicts those two data points in comparison to the temperature variation of the cubic lattice constant a of C_{60} crystals measured by Lubenets *et al.* [6]. Within the experimental uncertainty, both data sets are consistent. As one can infer, the cubic lattice constant of C_{60} amounts to $a = 14.05(1)$ Å at 77.6 K, and thus the nearest-neighbor distance is $d_{\text{NN,bulk}} = a/\sqrt{2} = 9.93(1)$ Å, which is about 0.8–0.9% smaller than the value used by Wang *et al.*

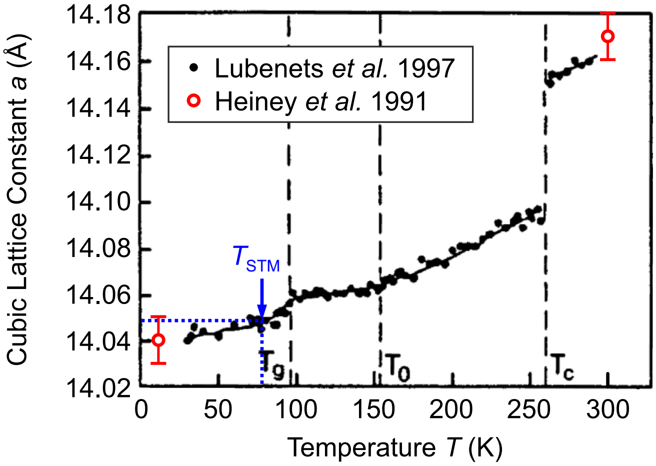

FIG. 2. Temperature variation of the cubic lattice constant a of C_{60} crystals (four molecules per unit cell), adapted from Ref. [6] with the permission of AIP Publishing. Values obtained for C_{60} powder are given as red open circles [5]. Within the experimental uncertainty of ±0.01 Å, both data sets are consistent. The blue dotted line is a guide to the eye. The cubic lattice constant amounts to $a = 14.05(1)$ Å at $T_{\text{STM}} = 77.6$ K.

The role of the substrate

The nominal thickness of 10–15 ML of cadmium corresponds to a physical thickness of ≈ 5–8 nm [11]. Thus, at least two *possible* scenarios for the Cd(0001) substrate should be considered:

Scenario (i): The Cd film produced in Ref. [1] behaves indeed bulklike. Due to the small thickness of the Cd film this assumption is not *a priori* justified; nevertheless, let us suppose for now that it is valid. Wang *et al.* cite a Cd lattice constant of $a = 2.97$ Å from Ref. [11]. It is rather likely that they have overlooked a necessary unit conversion. In the original paper by Edwards *et al.*, the historic kX units were used: $a = 2.9734(1)$ kX at 298 K [11]. The conversion factor of 1 kX = 1.002 02 Å needs to be applied [12,13], otherwise a systematic relative error of 0.2% occurs. The appropriately converted value is $a = 2.9794(1)$ Å. A more severe conceptual problem is that Ref. [11] only contains lattice constants of pure Cd for $T = 298$ K and above, but Wang *et al.* measured their structures at $T_{\text{STM}} = 77.6$ K [1]. Figure 3 depicts the thermal expansion coefficient $\alpha_\perp$ measured for cadmium crystals perpendicular to the hexagonal c-axis [14,15]. Based on these data, the extrapolation of the lattice constant yields $a = 2.969(2)$ Å at 77.6 K. The difference between the values at 298 and 77.6 K is significant, and the negligence of this effect introduces a systematic error of 0.3–0.4%. In this particular case, due to a fortuitous compensation of errors, the rounded value of $a = 2.97$ Å stated in Ref. [1] is rather close to the value of $a = 2.969(2)$ Å comprehensibly derived here [16].

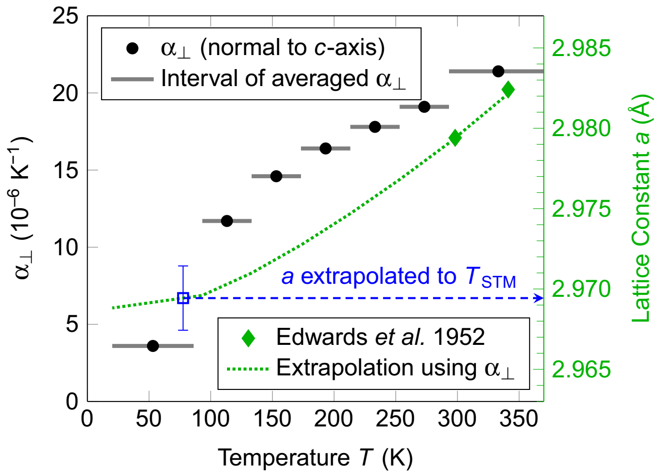

FIG. 3. Thermal expansion of Cd crystals perpendicular to the hexagonal c-axis [14]. The data points (solid circles) are averaged $\alpha_\perp$ values for the temperature intervals indicated by the gray horizontal bars [14,15]. On the right ordinate axis, the lattice constant a of Cadmium is plotted, where the data point at 298 K is $a_{\text{ref}} = 2.9794(1)$ Å [11]. The dotted line is the extrapolation of a based on $\alpha_\perp$ given here using $a_m - a_n = a_{\text{ref}}\,\alpha_\perp(T_m - T_n)$ as in Ref. [15]. If one assumes a relative uncertainty of 20% for $\alpha_\perp$, then the extrapolation of the lattice constant yields $a = 2.969(2)$ Å at $T_{\text{STM}} = 77.6$ K.

Scenario (ii): The Si(111)-(7 × 7) substrate acts as a template, thereby forming an epitaxial registry with the Cd film produced in Ref. [1], and there is no relaxation in 10–15 ML Cd films. If this epitaxial registry is fixed, then the Cd surface lattice likely follows the thermal expansion of the Si lattice. The (7 × 7) reconstruction of Si(111) is characterized by the substrate lattice vectors $\vec{s}_1$ and $\vec{s}_2$ with $|\vec{s}_1| = |\vec{s}_2| = 7a_{\mathrm{Si}}/\sqrt{2} = 26.876\,36(21)$ Å at 77.6 K. The unit cell angle is $\Gamma = \measuredangle(\vec{s}_1, \vec{s}_2) = 120\,^\circ$. Here, we used the cubic lattice constant $a_{\mathrm{Si}} = 5.429\,84(3)$ Å at 77.6 K extracted from measurements in a broad range of temperatures [17]. In this scenario, a plausible epitaxial interface would form if a 9 × 9 Cd overlayer structure were commensurate with the Si(111)-(7 × 7) substrate, resulting in a lattice constant of $a = 2.986\,26(2)$ Å for the average Cd(0001) unit cell at 77.6 K. This value is only about 0.6% larger than $a = 2.969(2)$ Å for scenario (i) and therefore indeed feasible. However, neither the epitaxial relation between Cd and Si nor its temperature dependence is elaborated on in Ref. [1]. Several reports revealed that Cd(0001) multilayer films are almost perfectly electronically transparent, i.e., the electron motion is highly anisotropic with a large lateral effective mass in (0001)-terminated Cd films [1,18]. Consequently, it appears to be rather challenging to simultaneously image the Si(111)-(7 × 7) substrate and the Cd film in the STM with sufficient resolution. Thus, for a determination of the epitaxial relation at this interface [experimental uncertainties lower than 0.6% are required to discriminate between scenarios (i) and (ii)], diffraction methods, such as distortion-corrected LEED [7], are advisable.

Scenarios (i) and (ii) are just two special cases for the Cd(0001) films. The structural behavior might even differ and should thus be examined more precisely if one aims for subpercent accuracy.

[1] Z. Wang, K. Sun, M. Tao, D. Yang, M. Shi, Z. Li, and J. Wang, Commensurate-incommensurate transition and strain relief patterns in monolayer C_{60} on Cd(0001), Phys. Rev. B **103**, 245430 (2021).
[2] C. Wagner, R. Forker, and T. Fritz, On the origin of the energy gain in epitaxial growth of molecular films, J. Phys. Chem. Lett. **3**, 419 (2012).
[3] R. Forker, M. Meissner, and T. Fritz, Classification of epitaxy in reciprocal and real space: Rigid versus flexible lattices, Soft Matter **13**, 1748 (2017).
[4] M. Meissner, F. Sojka, L. Matthes, F. Bechstedt, X. Feng, K. Müllen, S. C. B. Mannsfeld, R. Forker, and T. Fritz, Flexible 2D crystals of polycyclic aromatics stabilized by static distortion waves, ACS Nano **10**, 6474 (2016).
[5] P. A. Heiney, J. E. Fischer, A. R. McGhie, W. J. Romanow, A. M. Denenstein, J. P. McCauley, Jr., A. B. Smith, and D. E. Cox, Orientational Ordering Transition in Solid C_{60}, Phys. Rev. Lett. **66**, 2911 (1991).
[6] S. V. Lubenets, V. D. Natsik, L. S. Fomenko, A. P. Isakina, A. I. Prokhvatilov, M. A. Strzhemechny, N. A. Aksenova, and R. S. Ruoff, The structure, slip systems, and microhardness of C_{60} crystals, Low Temp. Phys. **23**, 251 (1997).
[7] F. Sojka, M. Meissner, C. Zwick, R. Forker, and T. Fritz, Determination and correction of distortions and systematic errors in low-energy electron diffraction, Rev. Sci. Instrum. **84**, 015111 (2013).
[8] C.-L. Hsu and W. W. Pai, Aperiodic incommensurate phase of a C_{60} monolayer on Ag(100), Phys. Rev. B **68**, 245414 (2003).
[9] C.-H. Lin, A. Huang, W. W. Pai, W.-C. Chen, T.-Y. Chen, T.-R. Chang, R. Yukawa, C.-M. Cheng, C.-Y. Mou, I. Matsuda, T.-C. Chiang, H.-T. Jeng, and S.-J. Tang, Single-layer dual germanene phases on Ag(111), Phys. Rev. Materials **2**, 024003 (2018).
[10] T.-Y. Chen, D. Mikolas, S. Chiniwar, A. Huang, C.-H. Lin, C.-M. Cheng, C.-Y. Mou, H.-T. Jeng, W. W. Pai, and S.-J. Tang, Germanene structure enhancement by adjacent insoluble domains of lead, Phys. Rev. Research **3**, 033138 (2021).
[11] D. E. Edwards, W. E. Wallace, and R. S. Craig, Magnesium-cadmium alloys. IV. The cadmium-rich alloys; some lattice parameters and phase relationships between 25 and 300°. Structure of the $MgCd_3$ superlattice. Schottky defects and the anomalous entropy, J. Am. Chem. Soc. **74**, 5256 (1952).
[12] W. L. Bragg and E. A. Wood, The conversion factor for kX units to Ångström units, J. Am. Chem. Soc. **69**, 2919 (1947).
[13] *American Institute of Physics Handbook*, edited by D. E. Gray (McGraw-Hill, New York, 1957), Chap. 2, p. 48.
[14] E. Grüneisen and E. Goens, Untersuchungen an Metallkristallen. III. Thermische Ausdehnung von Zink und Cadmium, Z. Phys. **29**, 141 (1924).
[15] Thermal expansion of technical solids at low temperatures, in *National Bureau of Standards Monograph 29*, edited by R. J. Corruccini and J. J. Gniewek (U.S. Government Printing Office, Washington, D.C., 1961), p. 16.
[16] We are not aware of any measurement of the Cd lattice constants at ≈78 K, which could be expected to significantly reduce the uncertainty in comparison to our extrapolation based on the thermal expansion coefficient.
[17] J. Potter, J. E. Parker, A. R. Lennie, S. P. Thompson, and C. C. Tang, Low-temperature Debye-Scherrer powder diffraction on Beamline I11 at Diamond, J. Appl. Crystallogr. **46**, 826 (2013).
[18] M.-L. Tao, H.-F. Xiao, K. Sun, Y.-B. Tu, H.-K. Yuan, Z.-H. Xiong, J.-Z. Wang, and Q.-K. Xue, Visualizing buried silicon atoms at the Cd-Si(111)-7 × 7 interface with localized electrons, Phys. Rev. B **96**, 125410 (2017).